European Journal of Medicinal Chemistry 106 (2015) 50–59

Contents lists available at ScienceDirect

European Journal of Medicinal Chemistry

journal homepage: http://www.elsevier.com/locate/ejmech

Research paper

Synthesis and biological evaluation of negative allosteric modulators of the K_v11.1(hERG) channel

Zhiyi Yu, Jacobus P.D. van Veldhoven, Ingrid M.E. 't Hart, Adrian H. Kopf, Laura H. Heitman, Adriaan P. IJzerman*

Division of Medicinal Chemistry, Leiden Academic Centre for Drug Research, Leiden University, 2300 RA Leiden, The Netherlands

ARTICLE INFO

Article history:
Received 12 August 2015
Received in revised form
14 October 2015
Accepted 16 October 2015
Available online 21 October 2015

Keywords:
K_v11.1(hERG) channel
Negative allosteric modulator
Radioligand binding assay
Antiarrhythmia
K_v11.1 blockers

ABSTRACT

We synthesized and evaluated a series of compounds for their allosteric modulation at the K_v11.1 (hERG) channel. Most compounds were negative allosteric modulators of [^{3}H]dofetilide binding to the channel, in particular **7f**, **7h**–**j** and **7p**. Compounds **7f** and **7p** were the most potent negative allosteric modulators amongst all ligands, significantly increasing the dissociation rate of dofetilide in the radioligand kinetic binding assay, while remarkably reducing the affinities of dofetilide and astemizole in a competitive displacement assay. Additionally, both **7f** and **7p** displayed peculiar displacement characteristics with Hill coefficients significantly distinct from unity as shown by e.g., dofetilide, further indicative of their allosteric effects on dofetilide binding. Our findings in this investigation yielded several promising negative allosteric modulators for future functional and clinical research with respect to their antiarrhythmic propensities, either alone or in combination with known K_v11.1 blockers.

1. Introduction

The past decades have witnessed an emerging interest in the identification of allosteric modulators of G protein-coupled receptors (GPCRs), ligand-gated ion channels (LGICs) and enzymes [1–3]. Allosteric modulators are ligands that bind to a binding site on a target protein that is not overlapping with and spatially distinct from the so-called orthosteric binding site, i.e. the site where e.g., hormones and neurotransmitters bind [4]. Negative allosteric modulators reduce receptor binding and/or function associated with orthosteric ligands, whereas positive allosteric modulators enhance these [2,4,5]. The therapeutic potential of allosteric modulators has been demonstrated in clinical trials, with a number of such drugs now on the market. Allosterically acting ligands provide novel opportunities for drug discovery due to a possible higher subtype-selectivity (allosteric sites are usually less conserved than orthosteric binding sites) and fewer side effects compared with traditional orthosteric compounds due to their 'ceiling' effect [2,3]. However, research on the allosteric modulation of voltage-gated ion channels (VGICs) is largely lacking, in particular for the K_v11.1 (hERG) channel.

The K_v11.1 channel, encoded by the human ether-à-go-go-related gene (hERG), plays a vital role in regulating cardiac repolarization of the action potential of human ventricular myocytes [6,7]. Genetic dysfunction or pharmacological inhibition of the K_v11.1 channel leads to prolongation of the action potential duration (APD), QT interval lengthening, and the development of Torsades de Pointes (TdP) [8]. A staggering array of drugs including antiarrhythmic agents, antihistamines, antibiotics and antipsychotics are known to block the K_v11.1 channel via a common, promiscuous binding region within the aqueous inner cavity of the pore [9,10]. More recently, a small number of compounds, referred to as K_v11.1 activators, have been proposed to remediate repolarization disorders in the heart, including acquired and congenital long QT syndromes, due to their up-regulation of K_v11.1 currents [7,11,12]. These activators were found to bind at sites that are distinct from each other and also different from the binding residues of prototypical K_v11.1 blockers [10]. For instance, RPR260243 ((3*R*,4*R*)-4-[3-(6-methoxyquinolin-4-yl)-3-oxopropyl]-1-[3-(2,3,5-trifluorophenyl)prop-2ynyl] piperi-dine-3-carboxylic acid) that was designated as a type 1 activator interacted with a putative binding site at the cytoplasmic end facing away from the inner

* Corresponding author.
E-mail address: ijzerman@lacdr.leidenuniv.nl (A.P. IJzerman).

http://dx.doi.org/10.1016/j.ejmech.2015.10.032
0223-5234/

cavity of the channel, while type 2 activators like NS1643 (1,3-bis[2-hydroxy-5-(trifluoromethyl)phenyl]urea) appeared to interact with residues located on the outer mouth of the pore [9,13,14]. Furthermore, some of these activators were found to reduce the affinities and subsequently reverse the action potential prolongation produced by K_v11.1 blockers. Pretreatment of cells expressing the K_v11.1 channel with RPR260243 slightly reduced the affinity of the reference hERG blocker dofetilide (*N*-[4-(2-{[2-(4-methane sulfonamidophenoxy)ethyl] (methyl) amino}ethyl)phenyl] methanesulfonamide), leading to a reduction of dofetilide's prolongation of the action potential [13,15]. Likewise, NS3623 (1-[4-bromo-2-(2*H*-tetrazol-5-yl)phenyl]-3-[3-(trifluoro-methyl)phenyl]urea) produced a reversal of E-4031 (*N*-[4-[[1-[2-(6-Methyl-2-pyridinyl) ethyl]-4-piperidinyl]carbonyl]phenyl]methanesulfonamide dihydrochloride)-induced QT prolongation in both anaesthetized and conscious guinea pigs [16] In this sense, the so-called activators might be negative allosteric modulators of the action of K_v11.1 blockers, and so normalize the pharmacologically induced action potential prolongation. Indeed, the allosteric terminology at the K_v11.1 channel has been introduced in our previous study and a recent review [4,17]. Classic methods for screening allosteric modulators have been based on techniques used to identify K_v11.1 blockers, such as voltage-dependent fluorescence experiments and laborious patch clamp assays. However, these methods do not allow high throughput screening in the search for new hit and lead molecules [18]. Moreover, although negative allosteric modulators of the K_v11.1 channel may be therapeutically promising, the current generation of modulators is not very potent and this raises concerns about their selectivity and liability for cardiac and non-cardiac side effects [10,12]. Therefore, it would be of particular importance to design and synthesize more novel allosteric modulators with higher potencies at the K_v11.1 channel.

Recently, Zhang et al. characterized a potent modulator (ML-T531 [19], compound **7a** in this study) for the K_v11.1 channel after screening a large compound library using an automated electrophysiological technique, and found that it normalized APD prolongation induced by dysfunction of the K_v7.1 channel [19]. This was the first experimental evidence that K_v11.1 modulators can prevent long QT type 1 (LQT1) in addition to type 2 (LQT2) syndrome. The concept that K_v7.1 and K_v11.1 activators can mutually rescue K_v7.1-related LQT1 and K_v11.1-induced LQT2 syndromes has been put forward previously, and was also validated by using a highly selective K_v7.1 modulator, R-L3 ((3*R*)-5-(2-fluorophenyl)-3-(1*H*-indol-3-ylmethyl)-1-methyl-3*H*-1,4-benzodiazepin-2-one)), which suppressed early after-depolarizations initiated by the K_v11.1 blocker dofetilide in rabbit myocytes [18,20,21]. Apart from ML-T531, a chemically similar compound (VU0405601 [22], compound **7r**) was discovered in a fluorescence-based thallium influx assay, and this ligand allosterically diminished the affinity of dofetilide at the channel and relieved the arrhythmia induced by dofetilide [22]. Altogether, negative allosteric modulators of the K_v11.1 channel could be beneficial in LQT syndromes induced by genetic loss-of-function or pharmacological inhibition of both K_v11.1 and K_v7.1 channels. In the present study, we selected ML-T531 and VU0405601 as our starting point, and synthesized a series of new ligands with modifications at the three aromatic rings present in the basic scaffold of the lead compounds. Based on the results from a previously validated single point dissociation assay [17], their structure–activity relationships were analyzed. Subsequently, a selection of potent negative allosteric modulators were comprehensively characterized in [^{3}H]dofetilide dissociation and displacement assays, and their influences on affinities of two specific K_v11.1 blockers (dofetildie and astemizole (1-[(4-fluorophenyl) methyl]-*N*-[1-[2-(4-methoxyphenyl)ethyl]-4-piperidyl]benzoimidazol-2-amine)) were evaluated as well.

2. Results and discussion

2.1. Chemistry

The synthetic route of all final compounds is depicted in Scheme 1 except that compound **7r** was synthesized as previously described [22]. Small systematic chemical variations were made by introducing different functional groups at the three aromatic rings of the reference compound (ML-T531, **7a**). Compounds based on modifications at the two phenyl rings (**7a**–**p**) were synthesized as follows. Friedel–Crafts acylation of substituted anisols (**1a**–**c**) and benzoyl chlorides (**2d**–**l** and **2n**–**p**) resulted in the formation of different substituted-benzophenone derivatives (**3b**–**l** and **3n**–**p**) [23]. Apart from acid chlorides **2o** and **2p** that were synthesized from the corresponding carboxylic acids **8o** and **8p** (Scheme S1, supporting information), all other intermediates were commercially available. Demethylation of the methoxy group for compounds **3b**–**l** and **3n**–**p** with $AlCl_3$ or BBr_3 in the case of **3c** led to **4b**–**l** and **4n**–**p** with high yields (65–97%) [23,24]. Notably, demethylation of **3c** using $AlCl_3$ conditions resulted in the undesired debrominated product **4a**. Subsequently, reaction of **4a**–**p** with 2-methylbromoacetate and hydrolysis of **5a**–**p** with LiOH produced compounds **6a**–**p**. Eventually, final compounds **7a**–**p** were obtained via a peptide coupling, using EDCI (1-Ethyl-3-(3-dimethylaminopropyl)carbodiimide)·HCl (**7e** and **7l**) or the superior HATU (1-[Bis(dimethylamino)methylene]-1H-1,2,3-triazolo [4,5-b]pyridinium-3-oxide hexafluorophosphate), between the acids (**6a**–**p**) and 3-aminopyridine in yields of 23–98% [22]. Fluorenone analogue **7q** was synthesized as follows: i) an oxidative dehydrogenative cyclization of benzophenone **4a** resulted in fluorenone intermediate **4q**, and ii) subsequent HATU peptide coupling conditions led to the formation of final compound **7q** [25]. To further investigate the influences of the 3-pyridine ring on the allosteric modulation capacities of ligands, a variety of substituted 3-aminopyridines (**7f1**–**f8**) and other nitrogen-containing heterocyclic rings (**7f9**–**f11**) were synthesized in a similar approach as described above. All intermediates were commercially available except intermediate **10f5**, which was synthesized from 5-bromo-3-methoxypyridine (**9f5**) through an amination using ammonia and copper sulfate pentahydrate (Scheme S1, supporting information) [26].

2.2. Structure–activity relationships

Initially, all synthesized compounds were tested for their abilities to increase or decrease the dissociation of [^{3}H]dofetilide from the HEK293K_v11.1 cell membrane preparations at 10 μM in a single point dissociation assay [17], and the results are summarized in Tables 1–3. Compound **7a**, also referred to as ML-T531 in literature, has been reported to be the most potent K_v11.1 activator, which normalizes the prolonged APDs of patient-derived cardiomyocytes [19]. Thus, a series of compounds with different substituents on the phenylcarbonyl ring were synthesized and evaluated for their allosteric modulation at the K_v11.1 channel (Table 1). Similar to compound **7a**, all compounds behaved as negative allosteric modulators of the K_v11.1 channel as they significantly increased the dissociation of dofetilide from the channel except **7l** and **7n**. The latter observation is in agreement with the previous finding that the effect of **7n** on K_v11.1 currents was insignificant and negligible [19], indicative of the reliability of our high-throughput single point dissociation assay. Introduction of halogens at the ortho position (**7d**, **7e** and **7g**) did not significantly impact the negative allosteric effect of the lead compound **7a**, whereas halogen substituents at the meta position (**7h**–**k**) displayed a more prominent enhancement of dofetilide dissociation compared to **7a**. Notably,

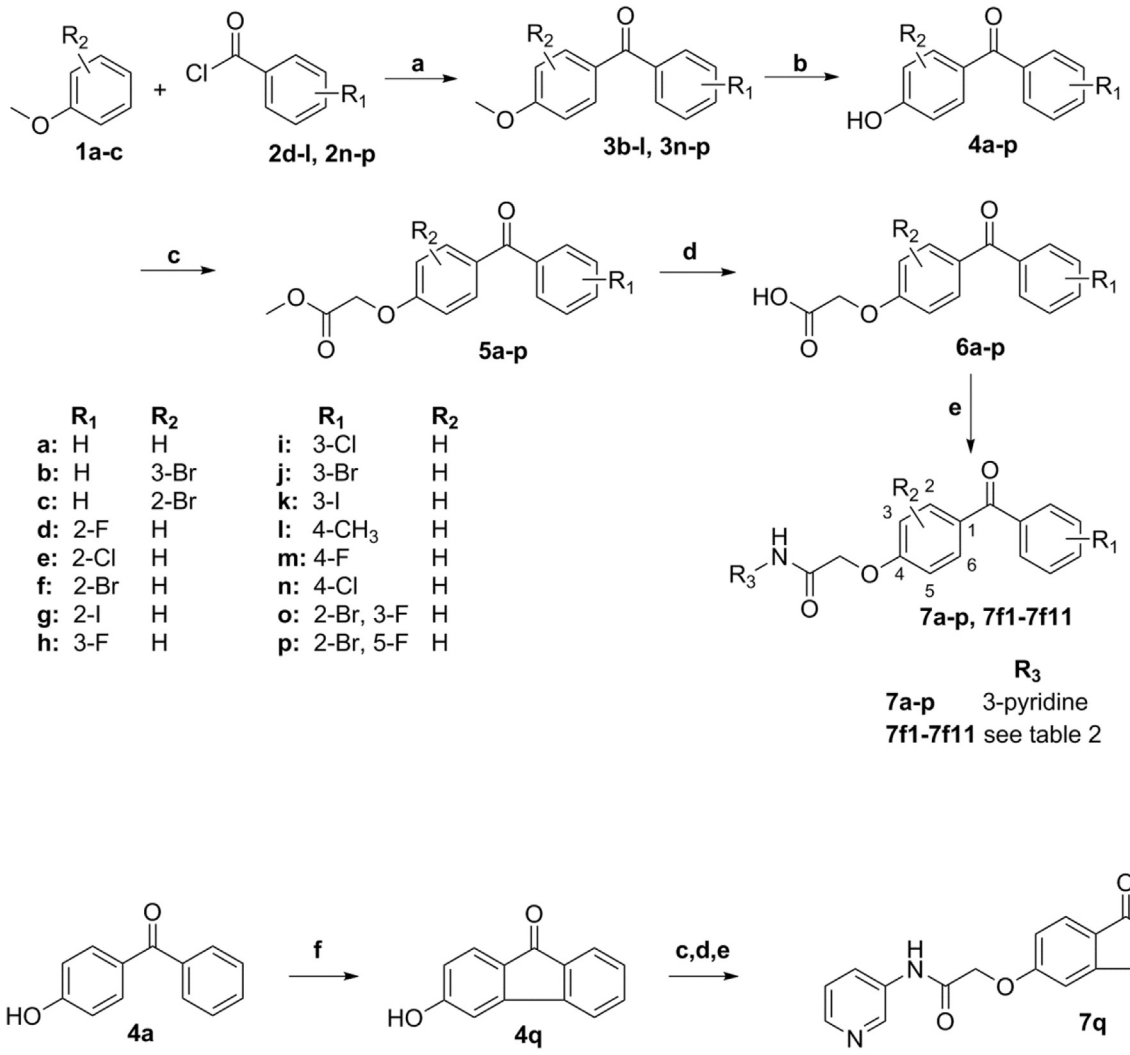

Scheme 1. Synthesis of compounds **7a**–**q** and **7f1**–**f11**. a) $AlCl_3$, DCM (dichloromethane), 0 °C to r.t., 2 h; b) $AlCl_3$, toluene, 130 °C, 2 h; c) 2-methylbromoacetate, K_2CO_3, DMF, 65 °C, overnight; d) LiOH, THF, MeOH, 105 °C, 30 min; e) 3-aminopyridine, Et_3N, HATU or EDCI·HCl (**7e** and **7l**), DMF, overnight.

Table 1
Allosteric modulation of [^{3}H]dofetilide binding at the K_v11.1 channel by 10 μM of compounds **7a** and **7d**–**p**. **%B/B$_{control}$** represents percentage specific binding of [^{3}H] dofetilide to the K_v11.1 channel after 6 min of dissociation induced by 10 μM dofetilide in the absence (**B$_{control}$**) or presence of 10 μM ligands (**B**).

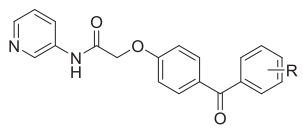

Compd	R	%B/B$_{control}$	Compd	R	%B/B$_{control}$
7a	H	78 ± 3	**7j**	3-Br	57 ± 5
7d	2-F	85 ± 4	**7k**	3-I	62 ± 3
7e	2-Cl	71 ± 2	**7l**	4-CH_3	97 ± 5
7f	2-Br	44 ± 1	**7m**	4-F	65 ± 2
7g	2-I	72 ± 2	**7n**	4-Cl	104 ± 2
7h	3-F	47 ± 2	**7o**	2-Br, 3-F	85 ± 1
7i	3-Cl	43 ± 2	**7p**	2-Br, 5-F	38 ± 3

introduction of a bromo substituent at the ortho position (**7f**) dramatically decreased the relative binding of dofetilide to 44 ± 1% from 78 ± 3% for **7a**, which implicated that ortho-bromo derivatives could be the starting point for designing more potent allosteric modulators of the K_v11.1 channel in the following step. With respect to the para position, methyl and chloro substituents (**7l** and **7n**) totally abolished the negative allosteric modulation properties of this series of compounds, while the 4-fluoro derivative slightly increased the allosteric effect (**7m** versus **7a**). The bigger size of the methyl and chloro substituents at the para-position may be the reason for this decrease in effect. Additionally, electron donating (**7l**) and withdrawing (**7n**) groups seemed to reduce the allosteric profiles of **7a** to the same extent, implying a negligible role of electronic effects in affecting allostery of compounds at the K_v11.1 channel. When bromo and fluoro substituents were simultaneously introduced to the ortho and meta positions, respectively, additional allosteric inhibition was observed for **7p** but **7o** exerted a much lower allosteric effect compared to compounds **7f** and **7h**. This confirms that steric hindrance at the phenyl ring might not be beneficial for the potency of these negative allosteric modulators.

Since compounds with a bromo substituent (**7f** and **7p**) at the ortho position of the phenylcarbonyl ring were among the most potent modulators, a variety of compounds with the same ortho-bromo substitution but different nitrogen-containing heterocyclic aromatic rings were designed to investigate the influences of the pyridine moiety on allosteric modulation of the K_v11.1 channel. As

Table 2
Allosteric modulation of [^{3}H]dofetilide binding at the K_v11.1 channel by 10 μM of compounds **7f1**–**f11**. **%B/B$_{control}$** represents percentage specific binding of [^{3}H] dofetilide to the K_v11.1 channel after 6 min of dissociation induced by 10 μM dofetilide in the absence (**B$_{control}$**) or presence of 10 μM ligands (**B**).

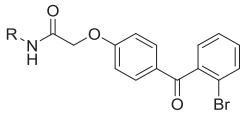

Compd	R	%B/B$_{control}$	Compd	R	%B/B$_{control}$
7f1		105 ± 12	**7f7**		105 ± 12
7f2		124 ± 13	**7f8**		87 ± 12
7f3	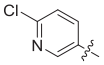	95 ± 12	**7f9**	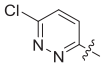	92 ± 2
7f4		121 ± 15	**7f10**		87 ± 9
7f5		107 ± 15	**7f11**		92 ± 2
7f6		108 ± 16			

displayed in Table 2, none of these compounds showed more prominent negative allosteric activities than the starting compound **7f**. By contrast, introduction of methyl, methoxyl, chlorine and phenyl groups amongst 3-pyridyl analogues (**7f1**–**f8**) abrogated the negative allosteric effects, and compounds **7f2** and **7f4** even appeared to decrease the dissociation of dofetilide albeit not significantly. It is worth noting that substituents with opposite electronic effects such as **7f1** and **7f3** could not be distinguished with respect to their allosteric activities, which is in agreement with our earlier finding for derivatives **7l** and **7n** shown in Table 1. This further proves that electronic effects were not the determinants of allosteric characteristics for this series of ligands. In addition, replacement of the pyridine ring with chlorine-substituted diazine (**7f9**), pyrimidine (**7f10**) and pyrazine (**7f11**) moieties led to significant decreases of the negative allosteric effects on the K_v11.1 channel compared to **7f**. Altogether, a non-substituted pyridine moiety is preferred for binding to the allosteric sites at the K_v11.1 channel. As compound **7r** (VU0405601) was found to significantly increase the IC_{70} value of dofetilide and thus prevent its K_v11.1 inhibition [22], substituents at the phenolic ring were also explored in Table 3. Introducing bromine at the phenolic ring wholly eliminated their allosteric effects (**7b**–**c** versus **7a**), whereby linkage of the two phenyl rings (**7q**) resulted in a comparably negative allosteric potency to the lead compound **7a**. Consistent with the previous publication [22], substitution of the general benzophenone moiety by a bromine-substituted naphthyl ring moderately increased the negative allosteric effect (**7r** versus **7a**).

Taken together, all three aromatic rings played critical roles in modifying the allosteric effects of this series of compounds at the K_v11.1 channel. In general, introducing halogen substituents with comparatively less steric hindrance at the phenylcarbonyl ring, and avoiding substituents at the pyridine and phenolic rings were favorable for enhancing the negative allosteric potencies of these modulators. Among all compounds shown in Tables 1–3, **7f**, **7i** and **7p** were the most potent negative allosteric modulators by reducing [^{3}H]dofetilide binding during dissociation to 44 ± 1, 43 ± 2 and 38 ± 3% respectively, which demonstrated their higher potencies than reference compounds **7a** (78 ± 3%) and **7r** (66 ± 3%).

Subsequently, several of the more potent allosteric modulators were selected in [^{3}H]dofetilide dissociation and displacement assays to exploit their pharmacological characteristics at the K_v11.1 channel in more detail. Since the disintegration characteristics of a radioligand–receptor complex can only be altered by the binding of a compound to a site distinct from the radioligand binding site, the effects of these synthesized compounds on the dissociation rate of [^{3}H]dofetilide can be unequivocally indicative of their allosteric actions [27]. In this respect, the dissociation behavior of [^{3}H]dofetilide was investigated in the absence (control) or presence of potent modulators (Table 4 and Fig. 1). As concentration-dependent allosteric modulation has been observed in a plethora of receptors [5,28–30], we evaluated a higher concentration (50 μM) of modulators in this assay, also to assess whether we could surpass the effects measured at 10 μM. The dissociation rate of the radioligand induced by an excess concentration of unlabeled dofetilide alone was 0.19 ± 0.01 min^{-1}, which was significantly increased by the selected compounds (**7f**, **7h**–**j** and **7p**), once more illustrating their negative allosteric modulation of the K_v11.1 channel. Compound **7p**

Table 3
Allosteric modulation of [^{3}H]dofetilide binding at the K_v11.1 channel by 10 μM of compounds **7b**, **7c**, **7q** and **7r**. **%B/B$_{control}$** represents percentage specific binding of [^{3}H] dofetilide to the K_v11.1 channel after 6 min of dissociation induced by 10 μM dofetilide in the absence (**B$_{control}$**) or presence of 10 μM ligands (**B**).

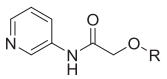

Compd	R	%B/B$_{control}$	Compd	R	%B/B$_{control}$
7b	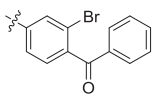	96 ± 1	**7q**	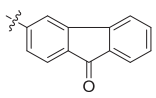	79 ± 6
7c	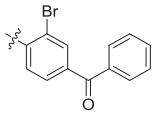	96 ± 7	**7r**	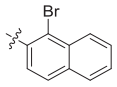	66 ± 3

Table 4
Dissociation rates of [^{3}H]dofetilide in the absence (control) or presence of 50 μM **7f**, **7h**–**j** and **7p**, and EC_{50} values of two representative compounds (**7f** and **7p**) at accelerating dissociation of [^{3}H]dofetilide from the K_v11.1 channel.

Compd	$k_{off,dofetilide}$ (min^{-1})	Fold	EC_{50} (μM)
Control	0.19 ± 0.01	–	–
+**7f**	0.57 ± 0.05***	3.0	12 ± 2
+**7h**	0.30 ± 0.04*	1.6	–
+**7i**	0.33 ± 0.03**	1.7	–
+**7j**	0.27 ± 0.03*	1.4	–
+**7p**	0.78 ± 0.20*	4.1	4.6 ± 0.4

Values are means (±SEM) of at least three independent experiments performed in duplicate (*P < 0.05, **P < 0.005, ***P < 0.001 versus control).

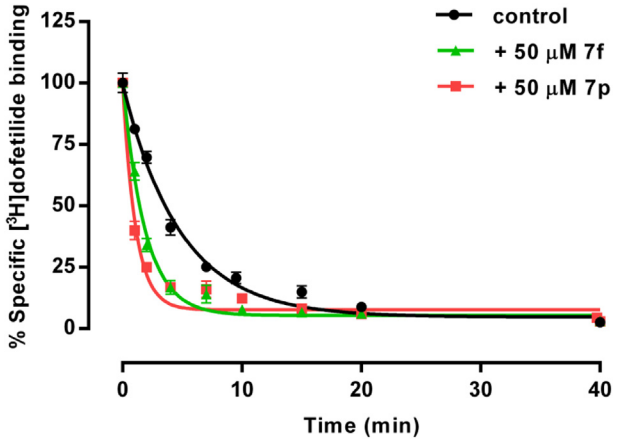

Fig. 1. Dissociation curves of [^{3}H]dofetilide by 10 μM dofetilide in the absence (control) or presence of 50 μM **7f** and **7p**. The experiment was performed at 25 °C with 20 μg HEK293K_v11.1 membranes. Data shown are from a representative experiment performed in duplicate.

was the most potent modulator that accelerated the k_{off} of dofetilide to 0.78 ± 0.20 min^{-1}, while **7j** was least efficacious with a dissociation rate of 0.27 ± 0.03 min^{-1} for dofetilide. The ranking order of all five compounds in enhancing the dissociation rate of dofetilde was identical to the one obtained in the single point dissociation assay except for compound **7f**, which had a more prominent negative allosteric action in this assay. Next, the concentration-dependent effects of two representative compounds at increasing the dissociation of [^{3}H]dofetilide from the K_v11.1 channel were assessed as in Fig. 2, and the determined EC_{50} values for **7f** and **7p** were 12 ± 2 and 4.6 ± 0.4 μM, respectively. This is in agreement with their activities in the other kinetic assays. It should be mentioned that a full concentration–effect curve of **7f** could not be recorded due to its limited solubility at higher concentrations. Furthermore, there was still 25% [^{3}H]dofetilide binding at the K_v11.1 channel left in the presence of 100 μM **7p**, which indicates that the binding of K_v11.1 blockers cannot be completely displaced via conformational changes of the channel caused by these negative allosteric modulators. More recently, curve-shifts that deviate from a simple competitive interaction at an equilibrium situation were revealed to be indicative of allostery [4]. Consequently, we determined the effect of the potent modulators (**7f**, **7h**–**j** and **7p**) on the equilibrium affinities of two prototypical K_v11.1 blockers, dofetilide and astemizole (Fig. 3 and Table 5). As shown in Fig. 3A and B, the displacement curves of both dofetilide and astemizole were rightward shifted by compound **7f** and **7p** at 10 μM, which is another indication of the negative allosteric properties of **7f** and **7p**. The affinities of dofetilide (K_i = 4.8 ± 0.5 nM) and astemizole (K_i = 1.3 ± 0.1 nM) were comparable to our previous findings [31],

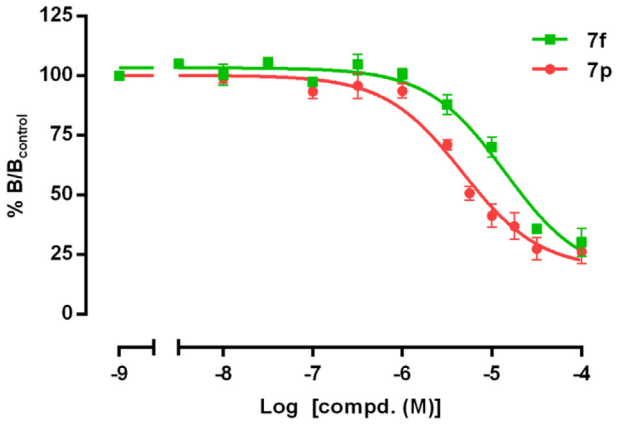

Fig. 2. Concentration-dependent effects of **7f** and **7p** in accelerating dissociation of [^{3}H]dofetilide from the K_v11.1 channel. Membrane proteins were first pre-equilibrated with [^{3}H]dofetilide, then the dissociation was induced by 10 μM dofetilide in the absence or presence of different concentrations of compounds and the incubation was terminated after 6 min. The results are expressed as the ratio of the specific binding of [^{3}H]dofetilide in the presence of 10 μM dofetilide plus various concentrations of negative allosteric modulators (B) over that in the presence of 10 μM dofetilide alone ($B_{control}$). The experiment was performed at 25 °C with 20 μg HEK293K_v11.1 membranes. Data shown are from a representative experiment performed in duplicate.

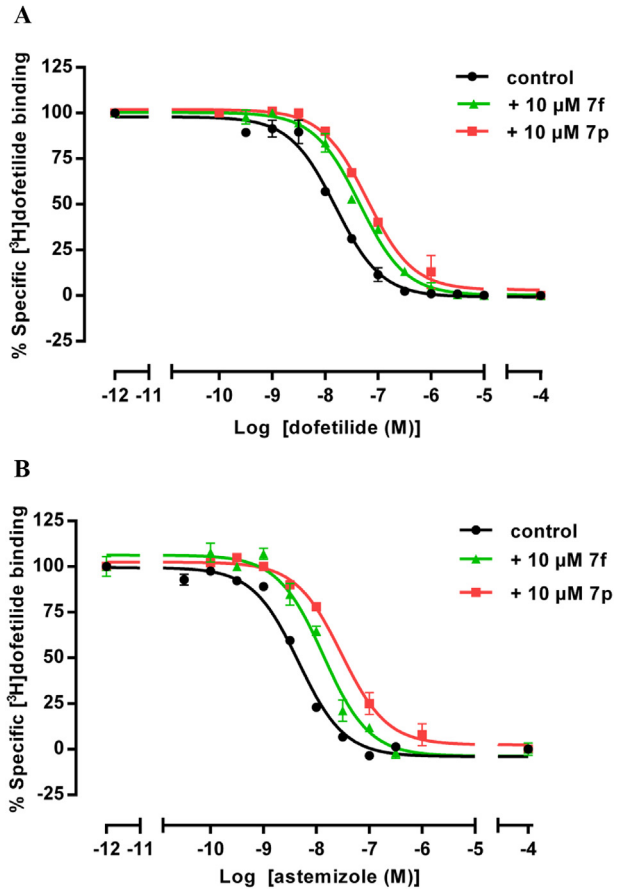

Fig. 3. Displacement curves of dofetilide (**A**) and astemizole (**B**) in the absence (control) or presence of 10 μM **7f** and **7p** in a [^{3}H]dofetilide binding assay. The experiment was performed at 25 °C with 20 μg HEK293K_v11.1 membranes. Data shown are from a representative experiment performed in duplicate.

and their apparent K_i values were increased in the presence of all tested compounds. The K_i values of dofetilide shifted to 6.8 ± 0.5 nM (**7j**) and 22 ± 5 nM (**7p**), while the values for

Table 5
The $K_v11.1$ affinities of dofetilide and astemizole in the absence (control) or presence of 10 μM **7f**, **7h**–**j** and **7p**.

Compd	$K_{i,\ dofetilide}$ (nM)	Fold	$K_{i,\ astemizole}$ (nM)	Fold
Control	4.8 ± 0.5	–	1.3 ± 0.1	–
+**7f**	12 ± 3*	2.5	5.3 ± 1.3*	4.1
+**7h**	8.9 ± 0.8*	1.9	2.5 ± 0.9	1.9
+**7i**	16 ± 4*	3.3	3.7 ± 0.1***	2.8
+**7j**	6.8 ± 0.5*	1.4	1.8 ± 0.5	1.4
+**7p**	22 ± 5*	4.6	8.2 ± 1.5*	6.3

Values are means (±SEM) of at least three independent experiments performed in duplicate (*P < 0.05, ***P < 0.001 versus control).

astemizole were 1.8 ± 0.5 nM (**7j**) and 8.2 ± 1.5 nM (**7p**). Apart from compound **7f**, the fold increase in K_i values for dofetilide and astemizole by these modulators was very comparable, and fully in line with our findings in the other dissociation assays. This diminishing of the affinities of $K_v11.1$ blockers through negative allosteric modulation is very appealing and may even help in mitigating acquired LQT syndromes via relieving drug-induced $K_v11.1$ blockade. The [^{3}H]dofetilide equilibrium displacement curves of **7f** and **7p** shown in Fig. 4 were rather steep with pseudo Hill coefficients (−1.8 for both compounds) much larger than unity, further indicating their allosteric actions on dofetilide binding at the $K_v11.1$ channel [30]. For the sake of comparison, the displacement curve of dofetilide was also included in Fig. 4, and the derived Hill slope was equal to −1.0 illustrating the competitive and 'orthosteric' binding of dofetilide and the reliability of this assay.

$K_v11.1$ activators have been introduced as a new potential antiarrhythmic strategy based on augmentation of the repolarization reserve of cardiomyocytes [32]. In this context, reference compounds **7a** and **7r** have also been defined as activators [19,22]. Compound **7r** had been found to decrease the affinities of $K_v11.1$ blockers dofetilide and droperidol, and to reduce the action potential prolongation by dofetilide in isolated rabbit ventricular cardiomyocytes. In a similar fashion, RPR26024, the first known $K_v11.1$ activator, dose-dependently reversed the action potential-prolonging effects of dofetilide in guinea pig myocytes [13]. We hypothesized that the $K_v11.1$ activators might exert their antiarrhythmic effects through negative allosteric modulation of the binding of $K_v11.1$ blockers to the channel, and verified that this was the case for compound **7r**. Additionally, compound **7a** had been found to relieve APD prolonged by a genetic dysfunction of the $K_v7.1$ channel [19]. Several negative allosteric modulators synthesized in this study displayed higher potencies than **7a** and **7r**, in particular **7f** and **7p**, which implicates their roles as lead compounds in eventually treating patients with LQT syndromes induced by pharmacological blockade of the $K_v11.1$ channel or due to genetic defects of the potassium channels.

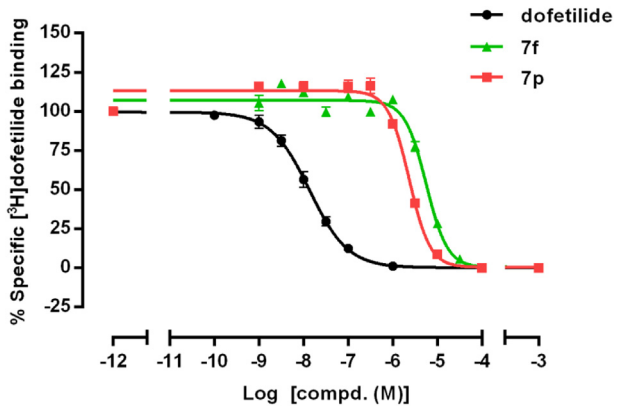

Fig. 4. Displacement curves of [^{3}H]dofetilide by dofetilide (control), **7f** and **7p**. The experiment was performed at 25 °C with 20 μg HEK293$K_v11.1$ membranes. Data shown are from a representative experiment performed in duplicate.

3. Conclusions

In summary, modifications of the three aromatic rings of the basic scaffold from reference compounds **7a** and **7r** lead to a series of compounds comprising of novel negative allosteric modulators of dofetilide binding to the $K_v11.1$ channel. Structure–activity relationships demonstrate that all the three aromatic rings play pivotal roles in determining the allosteric effects of these ligands at the $K_v11.1$ channel. Introducing halogen substituents at the meta-position of phenylcarbonyl ring together with non-substituted pyridine and phenolic rings enhances the negative allosteric effects of these modulators. In the kinetic dissociation assays, these compounds significantly accelerate the dissociation of [^{3}H]dofetilide from the $K_v11.1$ channel. Moreover, several potent modulators shift the displacement curves of prototypical $K_v11.1$ blockers (dofetilide and astemizole) to the right, and thus, diminish their $K_v11.1$ affinities at the channel. This is another indication of their negative allosteric properties, and also implicates their potential antiarrhythmic propensities in reducing acquired LQT syndromes induced by pharmacological blockade. Furthermore, these negative allosteric modulators may also become a new class of medicines for alleviating congenital LQT syndromes linked to both $K_v11.1$ and $K_v7.1$ channels like compound **7a**. Since compounds **7f** and **7p** are more potent than reference compounds **7a** and **7r**, they may serve as lead compounds for further optimization to relieve action potential prolongation through $K_v11.1$ channels or other potassium channels.

4. Experimental section

4.1. Chemistry

All solvents and reagents were purchased from commercial sources and were of analytical grade. Dematerialized water is simply referred to as H_2O, as was used in all cases unless stated otherwise (i.e. brine). ^{1}H and ^{13}C NMR spectra were recorded on a Bruker AV 400 liquid spectrometer (^{1}H NMR, 400 MHz; ^{13}C NMR, 100 MHz) at ambient temperature. Chemical shifts are reported in parts per million (ppm), are designated by δ and are downfield to the internal standard tetramethylsilane (TMS) in $CDCl_3$. Coupling-constants are reported in Hz and are designated as J. Analytical purity of the final compounds was determined by high pressure liquid chromatography (HPLC) with a Phenomenex Gemini 3 × C18 110A column (50 × 4.6 mm, 3 μm), measuring UV absorbance at 254 nm. Sample preparation and HPLC method was – unless stated otherwise – as follows: 0.3–0.8 mg of compound was dissolved in 1 mL of a 1:1:1 mixture of CH_3CN/H_2O/tBuOH and eluted from the column within 15 min, with a three component system of H_2O/CH_3CN/1% TFA in H_2O, decreasing polarity of the solvent mixture in time from 80/10/10 to 0/90/10. All compounds showed a single peak at the designated retention time and are at least 95% pure. Liquid chromatography–mass spectrometry (LC–MS) analyses were performed using Thermo Finnigan Surveyor – LCQ Advantage Max LC–MS system and a Gemini C18 Phenomenex column (50 × 4.6 mm, 3 μm). The sample preparation was the same as for HPLC analysis. The elution method was set up as follows: 1–4 min isocratic system of H_2O/CH_3CN/1% TFA in H_2O, 80:10:10, from the 4th min, a gradient was applied from 80:10:10 to 0:90:10 within 9 min, followed by 1 min of equilibration at 0:90:10 and 1 min at 80:10:10. Thin-layer chromatography (TLC) was routinely performed to monitor the progress

of reactions, using aluminum coated Merck silica gel F254 plates. Purification by column chromatography was achieved by use of Grace Davison Davisil silica column material (LC60A 30–200 micron). Solutions were concentrated using a Heidolph laborota W8 2000 efficient rotary evaporation apparatus and by a high vacuum on a Binder APT line Vacuum Drying Oven. Microwave reactions were carried out in a Biotage Initiator using sealed tubes and at a set reaction temperature. The procedure for a series of similar compounds is given as a general procedure for all within that series, annotated by the numbers of the compounds.

4.2. General peptide coupling method (*7a*–*r* and *7f1*–*f11*)

To a solution of **6a**–**r** (1.0 equiv.) and Et_3N (1.5 equiv.) in DMF (0.125 M) was added 3-aminopyridine (1.1 equiv.) and HATU (1.1 equiv.) or EDCI·HCl (**7e** and 7**l**). The mixture was stirred at room temperature for 20 h. The mixture was separated between ethyl acetate and water. The organic layer was washed with water twice, brine, dried over $MgSO_4$ and concentrated. Column chromatography using mixtures of 5% methanol/dichloromethane or EtOAc:Pet.ether 2:1 gave the pure desired products.

4.2.1. 2-(4-Benzoylphenoxy)-N-(pyridin-3-yl)acetamide (*7a*) [19]

White solid, 211 mg, yield = 69%. ^{1}H NMR (400 MHz, $CDCl_3$): δ 8.70 (s br, 1H), 8.44 (s br, 1H), 8.40 (s br, 1H), 8.22 (d, *J* = 8.0 Hz, 1H), 7.89 (d, *J* = 8.4 Hz, 2H), 7.77 (d, *J* = 7.6 Hz, 2H), 7.60 (t, *J* = 7.6 Hz, 1H), 7.50 (t, *J* = 7.6 Hz, 2H), 7.34 (d, *J* = 7.2 Hz, 1H), 7.09 (d, *J* = 8.8 Hz, 2H), 4.74 (s, 2H) ppm; ^{13}C NMR (101 MHz, $CDCl_3$): δ 195.3, 166.4, 160.2, 137.4, 132.4, 132.2, 131.2, 129.5, 128.1, 127.8, 114.1, 67.2 ppm; HPLC t_R = 7.28 min purity 100%; ESI-MS: 333.13 $[M+H]^+$.

4.2.2. 2-(4-Benzoyl-3-bromophenoxy)-N-(pyridin-3-yl)acetamide (*7b*)

White solid, 158 mg, yield = 51%. ^{1}H NMR (400 MHz, $CDCl_3$): δ 8.71 (s, 1H), 8.43 (d, *J* = 4.8 Hz, 2H), 8.24 (d, *J* = 8.0 Hz, 1H), 7.80 (d, *J* = 7.6 Hz, 2H), 7.61 (t, *J* = 7.6 Hz, 1H), 7.47 (t, *J* = 7.8 Hz, 2H), 7.39–7.31 (m, 3H), 7.03 (d, *J* = 8.4 Hz, 1H), 4.71 (s, 2H) ppm; HPLC t_R = 7.15 min purity 98%; ESI-MS: 411.13 $[M+H]^+$.

4.2.3. 2-(4-Benzoyl-2-bromophenoxy)-N-(pyridin-3-yl)acetamide (*7c*)

White solid, 293 mg, yield = 71%. ^{1}H NMR (400 MHz, $CDCl_3$): δ 8.80 (s, 1H), 8.74 (d, *J* = 2.4 Hz, 1H), 8.44 (d, *J* = 4.8 Hz, 1H), 8.27–8.23 (m, 1H), 8.15 (d, *J* = 1.6 Hz, 1H), 7.83 (dd, *J* = 8.4, 2.0 Hz, 1H), 7.80–7.74 (m, 2H), 7.63(t, *J* = 7.6 Hz, 1H), 7.52 (t, *J* = 7.6 Hz, 2H), 7.35 (dd, *J* = 8.4, 4.8 Hz, 1H), 7.00 (d, *J* = 8.8 Hz, 1H), 4.78 (s, 2H) ppm; HPLC t_R = 7.29 min purity 100%; ESI-MS: 411.07 $[M+H]^+$.

4.2.4. 2-[4-(2-Fluorobenzoyl)phenoxy]-N-(pyridin-3-yl)acetamide (*7d*)

White solid, 150 mg, yield = 78%. ^{1}H NMR (400 MHz, $CDCl_3$): δ 8.71 (s, 2H), 8.39 (d, *J* = 3.6 Hz, 1H), 8.20 (d, *J* = 8.0 Hz, 1H), 7.84 (d, *J* = 8.4 Hz, 2H), 7.55–7.49 (m, 2H), 7.31–7.24 (m, 2H), 7.15 (t, *J* = 8.4 Hz, 1H), 7.02 (d, *J* = 9.2 Hz, 2H), 4.70 (s, 2H) ppm; HPLC t_R = 6.67 min purity 98%; ESI-MS: 351.13 $[M+H]^+$.

4.2.5. 2-[4-(2-Chlorobenzoyl)phenoxy]-N-(pyridin-3-yl)acetamide (*7e*)

Used EDCI·HCl instead of HATU. White solid, 72 mg, yield = 20%. ^{1}H NMR (400 MHz, $CDCl_3$): δ 8.70–8.60 (m, 2H), 8.39 (d, *J* = 4.4 Hz, 1H), 8.19 (d, *J* = 8.0 Hz, 1H), 7.81 (d, *J* = 8.4 Hz, 2H), 7.45–7.28 (m, 5H), 7.02 (d, *J* = 8.4 Hz, 2H), 4.71 (s, 2H) ppm; HPLC t_R = 7.04 min purity 100%; ESI-MS: 367.13 $[M+H]^+$.

4.2.6. 2-[4-(2-Bromobenzoyl)phenoxy]-N-(pyridin-3-yl)acetamide (*7f*)

White solid, 9 mg, yield = 23%. ^{1}H NMR (400 MHz, $CDCl_3$): δ 8.68 (d, *J* = 2.0 Hz, 1H), 8.42 (d, *J* = 4.4 Hz, 1H), 8.36 (s, 1H), 8.22 (dt, *J* = 8.4, 0.8 Hz, 1H), 7.85 (d, *J* = 8.8 Hz, 2H), 7.65 (dd, *J* = 7.6, 0.8 Hz, 1H), 7.43 (td, *J* = 7.4, 1.2 Hz, 1H), 7.38–7.31 (m, 3H), 7.06 (d, *J* = 8.8 Hz, 2H), 4.72 (s, 2H) ppm; ^{13}C NMR (101 MHz, $CDCl_3$): δ 194.5, 166.0, 161.0, 146.1, 141.7, 140.6, 133.7, 133.3, 132.9, 131.3, 130.8, 128.9, 127.7, 127.4, 123.8, 119.5, 114.8, 67.5 ppm; HPLC t_R = 7.09 min purity 98%; ESI-MS: 411.07 $[M+H]^+$.

4.2.7. 2-[4-(2-Iodobenzoyl)phenoxy]-N-(pyridin-3-yl)acetamide (*7g*)

White solid, 113 mg, yield = 63%. ^{1}H NMR (400 MHz, $CDCl_3$): δ 8.68 (s, 1H), 8.43 (d, *J* = 4.4 Hz, 1H), 8.34 (s, 1H), 8.23 (d, *J* = 8.4 Hz, 1H), 7.93 (d, J = 8.0 Hz, 1H), 7.85 (d, *J* = 8.4 Hz, 2H), 7,46 (t, *J* = 7.6 Hz, 1H), 7.33 (dd, *J* = 8.4 Hz, 4.8 Hz, 1H), 7.29 (d, *J* = 7.6 Hz, 1H), 7.20 (td, *J* = 7.6 Hz, 1.2 Hz, 1H), 7.07 (d, *J* = 8.8 Hz, 2H), 4.73 (s, 2H) ppm; HPLC t_R = 7.19 min purity 100%; ESI-MS: 459.00 $[M+H]^+$.

4.2.8. 2-[4-(3-Fluorobenzoyl)phenoxy]-N-(pyridin-3-yl)acetamide (*7h*)

White solid, 80 mg, yield = 67%. ^{1}H NMR (400 MHz, $CDCl_3$): δ 8.83 (s, 1H), 8.73 (d, *J* = 2.4 Hz, 1H), 8.39 (d, *J* = 4.0 Hz, 1H), 8.21 (d, *J* = 8.8 Hz, 1H), 7.82 (d, *J* = 8.8 Hz, 2H), 7.52–7.42 (m, 3H), 7.32–7.27 (m, 2H), 7.04 (d, *J* = 8.8 Hz, 2H), 4.73 (s, 2H) ppm; ^{13}C NMR (101 MHz, $CDCl_3$): δ 193.9, 166.1, 163.8, 161.4, 160.4, 146.1, 141.6, 140.0, 139.9, 133.7, 132.8, 131.6, 130.2, 130.1, 127.8, 125.7, 125.6, 124.0, 119.5, 119.3, 116.8, 116.6, 114.7, 67.5 ppm; HPLC t_R = 6.88 min purity 100%; ESI-MS: 351.13 $[M+H]^+$.

4.2.9. 2-[4-(3-Chlorobenzoyl)phenoxy]-N-(pyridin-3-yl)acetamide (*7i*)

White solid, 319 mg, yield = 87%. ^{1}H NMR (400 MHz, $CDCl_3$): δ 8.72 (d, *J* = 2.0 Hz, 1H), 8.44–8.40 (m, 2H), 8.27 (dd, *J* = 8.4, 2.0 Hz, 1H), 7.88 (d, *J* = 8.8 Hz, 2H), 7.74 (t, *J* = 1.6 Hz, 1H), 7.63 (dt, *J* = 7.6, 1.6 Hz, 1H), 7.58–7.55 (m, 1H), 7.44 (t, *J* = 7.6 Hz, 1H), 7.36 (dd, *J* = 8.4, 4.8 Hz, 1H), 7.11 (d, *J* = 8.8 Hz, 2H), 4.75 (s, 2H) ppm; ^{13}C NMR (101 MHz, $CDCl_3$): δ 193.9, 166.1, 160.4, 146.2, 141.7, 139.5, 134.7, 133.7, 132.8, 132.3, 131.4, 129.8, 129.7, 127.9, 127.7, 123.9, 114.7, 67.5 ppm; HPLC t_R = 7.33 min purity 100%; ESI-MS: 367.07 $[M+H]^+$.

4.2.10. 2-[4-(3-Bromobenzoyl)phenoxy]-N-(pyridin-3-yl)acetamide (*7j*)

White solid, 63 mg, yield = 25%. ^{1}H NMR (400 MHz, DMSO): δ 10.42 (d, 1H), 8.79 (d, *J* = 2.0 Hz, 1H), 8.30 (d, *J* = 4.0 Hz, 1H), 8.07 (d, *J* = 8.4 Hz, 1H), 7.85 (d, *J* = 8.0 Hz, 1H), 7.81 (s, 1H), 7.78 (d, *J* = 8.8 Hz, 2H), 7.67 (d, *J* = 8.0 Hz, 1H), 7.51 (t, *J* = 7.6 Hz, 1H), 7.39–7.36 (m, 1H), 7.18 (d, *J* = 8.8 Hz, 2H), 4.90 (s, 2H) ppm; ^{13}C NMR (101 MHz, $CDCl_3$): δ 193.8, 166.0, 160.4, 146.3, 141.6, 139.8, 135.3, 133.7, 132.9, 132.7, 131.5, 130.1, 128.4, 127.7, 123.9, 122.7, 114.7, 67.5 ppm; HPLC t_R = 7.42 min purity 98%; ESI-MS: 411.13 $[M+H]^+$.

4.2.11. 2-[4-(3-Iodobenzoyl)phenoxy]-N-(pyridin-3-yl)acetamide (*7k*)

White solid, 91 mg, yield = 71%. ^{1}H NMR (400 MHz, DMSO): δ 8.79 (d, *J* = 2.4 Hz, 1H), 8.30 (dd, *J* = 4.8, 1.2 Hz, 1H), 8.07 (dt, *J* = 8.0, 1.6 Hz, 1H), 8.01 (d, *J* = 8.0 Hz, 1H), 7.98 (t, *J* = 1.2 Hz, 1H), 7.77 (d, *J* = 8.8 Hz, 2H), 7.68 (d, *J* = 7.6 Hz, 1H), 7.39–7.33 (m, 2H), 7.17 (d, *J* = 8.8 Hz, 2H), 4.89 (s, 2H) ppm; HPLC t_R = 7.50 min purity 98%; ESI-MS: 459.07 $[M+H]^+$.

4.2.12. 2-[4-(4-Methylbenzoyl)phenoxy]-N-(pyridin-3-yl) acetamide (*7l*)

Used EDCI·HCl instead of HATU. White solid, 81 mg, yield = 26%.

^{1}H NMR (400 MHz, $CDCl_3$): δ 8.69 (d, J = 1.6 Hz, 1H), 8.45–8.38 (m, 2H), 8.23 (dd, J = 7.2, 1.2 Hz, 1H), 7.85 (d, J = 8.8 Hz, 2H), 7.68 (d, J = 8.0 Hz, 2H), 7.33 (dd, J = 8.4, 4.8 Hz, 1H), 7.28 (d, J = 7.2 Hz, 2H), 7.07 (d, J = 8.8 Hz, 2H), 4.73 (s, 2H), 2.45 (s, 3H) ppm; HPLC t_R = 7.09 min purity 98%; ESI-MS: 347.13 $[M+H]^+$.

4.2.13. 2-(4-(4-Fluorobenzoyl)phenoxy)-N-(pyridin-3-yl)acetamide (**7m**)

White solid, 187 mg, yield = 53%. ^{1}H NMR (400 MHz, $CDCl_3$): δ 8.72 (d, J = 2.4 Hz, 1H), 8.44–8.40 (m, 2H), 8.30–8.23 (m, 1H), 7.85 (d, J = 8.8 Hz, 2H), 7.83–7.77 (m, 2H), 7.35 (dd, J = 8.4, 4.8 Hz, 1H), 7.17 (t, J = 8.8 Hz, 2H), 7.09 (d, J = 8.8 Hz, 2H), 4.74 (s, 2H) ppm; HPLC t_R = 6.89 min purity 99%; ESI-MS: 351.13 $[M+H]^+$.

4.2.14. 2-[4-(4-Chlorobenzoyl)phenoxy]-N-(pyridin-3-yl)acetamide (**7n**) [19]

White solid, 903 mg, yield = 98%. ^{1}H NMR (400 MHz, DMSO): δ 10.41 (s, 1H), 8.79 (d, J = 2.4 Hz, 1H), 8.30 (dd, J = 4.4, 1.2 Hz, 1H), 8.07 (dt, J = 8.0, 1.6 Hz, 1H), 7.77 (d, J = 8.8 Hz, 2H), 7.72 (dd, J = 8.8, 2.0 Hz, 2H), 7.62 (d, J = 8.4 Hz, 2H), 7.38 (dd, J = 8.4, 4.8 Hz, 1H), 7.17 (d, J = 8.8 Hz, 2H), 4.89 (s, 2H) ppm; HPLC t_R = 7.27 min purity 100%; ESI-MS: 367.13 $[M+H]^+$.

4.2.15. 2-[4-(2-Bromo-3-fluorobenzoyl)phenoxy]-N-(5-methoxypyridin-3-yl)acetamide (**7o**)

White solid, 69 mg, yield = 25%. ^{1}H NMR (400 MHz, $CDCl_3$): δ 8.68 (d, J = 2.0 Hz, 1H), 8.42 (d, J = 4.4 Hz, 1H), 8.37 (s, 1H), 8.22 (d, J = 8.4 Hz, 1H), 7.85 (d, J = 8.4 Hz, 2H), 7.44–7.39 (m, 1H), 7.33 (dd, J = 8.2, 4.8 Hz, 1H), 7.26 (t, J = 8.0 Hz, 1H), 7.13 (d, J = 7.6 Hz, 1H), 7.07 (d, J = 8.8 Hz, 2H), 4.72 (s, 2H) ppm; HPLC t_R = 7.25 min purity 98%; ESI-MS: 429.07 $[M+H]^+$.

4.2.16. 2-[4-(2-Bromo-5-fluorobenzoyl)phenoxy]-N-(5-methoxypyridin-3-yl)acetamide (**7p**)

White solid, 108 mg, yield = 39%. ^{1}H NMR (400 MHz, $CDCl_3$): δ 8.67 (s, 1H), 8.43 (d, J = 4.4 Hz, 1H), 8.28 (s, 1H), 8.21 (d, J = 8.4 Hz, 1H), 7.86 (d, J = 8.8 Hz, 2H), 7.61 (dd, J = 8.4, 4.8 Hz, 1H), 7.33 (dd, J = 8.0, 4.8 Hz, 1H), 7.14–7.03 (m, 4H), 4.73 (s, 2H) ppm; ^{13}C NMR (101 MHz, $CDCl_3$): δ 192.9, 165.9, 162.9, 161.3, 160.4, 146.1, 142.1, 141.7, 134.9, 134.8, 133.7, 132.9, 130.1, 127.7, 123.8, 118.7, 118.4, 116.2, 116.0, 114.9, 113.7, 67.5 ppm; HPLC t_R = 7.22 min purity 100%; ESI-MS: 429.07 $[M+H]^+$.

4.2.17. 2-[(9-Oxo-9H-fluoren-3-yl)oxy]-N-(pyridin-3-yl)acetamide (**7q**)

Started from **4q** and 3-aminopyridine. Yellow solid, 170 mg, yield = 51%. ^{1}H NMR (400 MHz, DMSO): δ 10.52 (s, 1H), 8.89 (d, J = 2.4 Hz, 1H), 8.37 (dd, J = 4.8, 1.2 Hz, 1H), 8.17 (d, J = 8.4 Hz, 1H), 7.81 (d, J = 7.2 Hz, 1H), 7.65–7.55 (m, 3H), 7.53–7.47 (m, 2H), 7.39(t, J = 7.2 Hz, 1H), 6.95 (dd, J = 8.0, 2.0 Hz, 1H), 4.95 (s, 2H) ppm; HPLC t_R = 6.73 min purity 99%; ESI-MS: 331.07 $[M+H]^+$.

4.2.18. 2-[(1-Bromonaphthalen-2-yl)oxy]-N-(pyridin-3-yl) acetamide (**7r**) [22]

White solid, 235 mg, yield = 74%. ^{1}H NMR (400 MHz, $CDCl_3$): δ 9.07 (s br, 1H), 8.77 (d, J = 2.4 Hz, 1H), 8.42 (dd, J = 4.8, 1.2 Hz, 1H), 8.28 (ddd, J = 8.4 Hz, 1.2, 1.2 Hz, 1H), 8.24 (d, J = 8.8 Hz, 1H), 7.89 (d, J = 8.8 Hz, 1H), 7.84 (d, J = 8.0 Hz, 1H), 7.65 (dd, J = 6.8, 0.8 Hz, 1H), 7.49 (dd, J = 7.2, 0.8 Hz, 1H), 7.34 (dd, J = 8.4, 3.6 Hz, 1H), 7.25 (d, J = 8.4 Hz, 1H), 4.83 (s, 2H); ^{13}C NMR (101 MHz, $CDCl_3$): δ 166.2, 151.2, 145.9, 141.4, 134.0, 132.8, 130.6, 129.8, 128.4, 128.3, 127.0, 126.3, 125.5, 123.8, 114.7, 109.9, 69.0 ppm. HPLC t_R = 7.95 min purity 99%; ESI-MS: 357.00 $[M+H]^+$.

4.2.19. 2-[4-(2-Bromobenzoyl)phenoxy]-N-(6-methylpyridin-3-yl) acetamide (**7f1**)

Started from **6f** and 5-amino-2-methylpyridine. White solid, 47 mg, yield = 73%. ^{1}H NMR (400 MHz, $CDCl_3$): δ 8.54 (d, J = 2.4 Hz, 1H), 8.35 (s, 1H), 8.07 (dd, J = 8.4, 2.4 Hz, 1H), 7.84 (d, J = 8.8 Hz, 2H), 7.65 (d, J = 7.6 Hz, 1H), 7.43 (td, J = 7.2, 0.8 Hz, 1H), 7.37–7.33 (m, 2H), 7.17 (d, J = 8.4 Hz, 1H), 7.05 (d, J = 8.8 Hz, 2H), 4.70 (s, 2H), 2.54 (s, 3H) ppm; HPLC t_R = 7.09 min purity 99%; ESI-MS: 425.07 $[M+H]^+$.

4.2.20. 2-[4-(2-Bromobenzoyl)phenoxy]-N-(6-methoxypyridin-3-yl)acetamide (**7f2**)

Started from **6f** and 5-amino-2-methoxypyridine. White solid, 50 mg, yield = 94%. ^{1}H NMR (400 MHz, $CDCl_3$): δ 8.31–8.20 (m, 2H), 7.91 (dd, J = 7.8, 2.0 Hz, 1H), 7.83 (d, J = 8.4 Hz, 2H), 7.64 (d, J = 7.6 Hz, 1H), 7.42 (t, J = 7.2 Hz, 1H), 7.37–7.32 (m, 2H), 7.04 (d, J = 8.8 Hz, 2H), 6.75 (d, J = 8.8 Hz, 1H), 4.69 (s, 2H), 3.92 (s, 3H) ppm; HPLC t_R = 9.06 min purity 98%; ESI-MS: 441.07 $[M+H]^+$.

4.2.21. 2-[4-(2-Bromobenzoyl)phenoxy]-N-(6-chloropyridin-3-yl) acetamide (**7f3**)

Started from **6f** and 5-amino-2-chloropyridine. Yellow solid, 51 mg, yield = 82%. ^{1}H NMR (400 MHz, $CDCl_3$): δ 8.47 (d, J = 2.8 Hz, 1H), 8.30 (s, 1H), 8.21 (dd, J = 8.8, 2.8 Hz, 1H), 7.85 (d, J = 8.0 Hz, 2H), 7.65 (d, J = 8.0 Hz, 1H), 7.43–7.32 (m, 4H), 7.05 (d, J = 8.8 Hz, 2H), 4.71 (s, 2H) ppm; HPLC t_R = 9.65 min purity 100%; ESI-MS: 445.07 $[M+H]^+$.

4.2.22. 2-[4-(2-Bromobenzoyl)phenoxy]-N-(5-methylpyridin-3-yl) acetamide (**7f4**)

Started from **6f** and 3-amino-5-methylpyridine. White solid, 55 mg, yield = 86%. ^{1}H NMR (400 MHz, $CDCl_3$): δ 8.47 (d, J = 2.0 Hz, 1H), 8.40 (s, 1H), 8.24 (s, 1H), 8.04 (s, 1H), 7.83 (dd, J = 7.8, 2.0 Hz, 2H), 7.65 (dd, J = 7.2, 0.8 Hz, 1H), 7.43 (td, J = 7.0, 1.2 Hz, 1H), 7.37–7.33 (m, 2H), 7.05 (d, J = 8.8 Hz, 2H), 4.71 (s, 2H), 2.36 (s, 3H) ppm. HPLC t_R = 7.18 min purity 99%; ESI-MS: 425.07 $[M+H]^+$.

4.2.23. 2-[4-(2-Bromobenzoyl)phenoxy]-N-(5-methoxypyridin-3-yl)acetamide (**7f5**)

Started from **6f** and 3-amino-5-methoxypyridine. White solid, 274 mg, yield = 100%. ^{1}H NMR (400 MHz, $CDCl_3$): δ 8.78 (s, 1H), 8.23 (d, J = 1.6 Hz, 1H), 8.09 (d, J = 2.4 Hz, 1H), 7.90 (t, J = 2.4 Hz, 1H), 7.80 (dt, J = 9.2, 2.0 Hz, 2H), 7.63 (dd, J = 7.8, 1.2 Hz, 1H), 7.41 (td, J = 7.8, 1.2 Hz, 1H), 7.34 (td, J = 7.8, 2.0 Hz, 1H), 7.30 (dd, J = 7.6, 2.0 Hz, 1H), 7.02 (dt, J = 8.8, 2.4 Hz, 2H), 4.70 (s, 2H), 3.85 (s, 3H) ppm. HPLC t_R = 7.44 min purity 99%; ESI-MS: 441.07 $[M+H]^+$.

4.2.24. 2-[4-(2-Bromobenzoyl)phenoxy]-N-(4-methylpyridin-3-yl) acetamide (**7f6**)

Started from **6f** and 3-amino-4-methylpyridine. White solid, 90 mg, yield = 70%. ^{1}H NMR (400 MHz, $CDCl_3$): δ 8.92 (s, 1H), 8.34 (d, J = 4.4 Hz, 1H), 8.28 (s, 1H), 7.84 (d, J = 8.8 Hz, 2H), 7.64 (d, J = 7.6 Hz, 1H), 7.43 (td, J = 7.2, 0.8 Hz, 1H), 7.35 (td, J = 7.8, 2.0 Hz, 1H), 7.33 (dd, J = 7.4, 2.0 Hz, 1H), 7.16 (d, J = 4.8 Hz, 1H), 7.05 (d, J = 8.8 Hz, 2H), 4.76 (s, 2H), 2.25 (s, 3H) ppm. HPLC t_R = 7.05 min purity 100%; ESI-MS: 425.13 $[M+H]^+$.

4.2.25. 2-[4-(2-Bromobenzoyl)phenoxy]-N-(4-methoxypyridin-3-yl)acetamide (**7f7**)

Started from **6f** and 3-amino-4-methoxypyridine. Yellow solid, 35 mg, yield = 72%. ^{1}H NMR (400 MHz, $CDCl_3$): δ 9.48 (s, 1H), 8.66 (s, 1H), 8.33 (d, J = 5.2 Hz, 1H), 7.85 (d, J = 8.8 Hz, 2H), 7.65 (d, J = 8.0 Hz, 1H), 7.44–7.32 (m, 3H), 7.05 (d, J = 8.8 Hz, 2H), 6.85 (d, J = 5.6 Hz, 1H), 4.72 (s, 2H), 3.95 (s, 3H) ppm. HPLC t_R = 7.13 min purity 99%; ESI-MS: 441.13 $[M+H]^+$.

*4.2.26. 2-(4-(2-Bromobenzoyl)phenoxy)-N-(quinolin-3-yl) acetamide (**7f8**)*

Started from **6f** and 3-aminoquinoline. White solid, 44 mg, yield = 83%. ^{1}H NMR (400 MHz, $CDCl_3$): δ 8.85 (d, J = 2.4 Hz, 1H), 8.79 (s, 1H), 8.60 (s, 1H), 8.06 (d, J = 8.4 Hz, 1H), 7.86–7.81 (m, 3H), 7.68–7.63 (m, 2H), 7.55 (t, J = 8.0 Hz, 1H), 7.40 (t, J = 7.6 Hz, 1H), 7.37–7,31 (m, 2H), 7.07 (d, J = 7.6 Hz, 2H), 4.76 (s, 2H) ppm. HPLC t_R = 8.10 min purity 99%; ESI-MS: 461.07 $[M+H]^+$.

*4.2.27. 2-[4-(2-Bromobenzoyl)phenoxy]-N-(6-chloropyridazin-3-yl)acetamide (**7f9**)*

Started from **6f** and 3-amino-6-chloro-pyridazine. White solid, 32 mg, yield = 6%. ^{1}H NMR (400 MHz, $CDCl_3$): δ 9.49 (s, 1H), 8.57 (d, J = 8.8 Hz, 1H), 7.86 (d, J = 7.6 Hz, 2H), 7.65 (d, J = 8.0 Hz, 1H), 7.57 (d, J = 9.2 Hz, 1H), 7.43–7.30 (m, 3H), 7.07 (d, J = 7.1 Hz, 2H), 4.77 (s, 2H) ppm. HPLC t_R = 9.37 min purity 97%; ESI-MS: 445.93 $[M+H]^+$.

*4.2.28. 2-[4-(2-Bromobenzoyl)phenoxy]-N-(pyrimidin-5-yl) acetamide (**7f10**)*

Started from **6f** and 5-aminopyrimidine. White solid, 24 mg, yield = 26%. ^{1}H NMR (400 MHz, $CDCl_3$): δ 9.08 (s, 2H), 9.03 (s, 1H), 8.45 (s, 1H), 7.81 (d, J = 8.8 Hz, 2H), 7.65 (d, J = 8.0 Hz, 1H), 7.43 (td, J = 7.4, 1.2 Hz, 1H), 7.39–7.31 (m, 2H), 7.05 (d, J = 8.8 Hz, 2H), 4.75 (s, 2H) ppm. HPLC t_R = 8.27 min purity 99%; ESI-MS: 412.07 $[M+H]^+$.

*4.2.29. 2-(4-(2-Bromobenzoyl)phenoxy)-N-(pyrazin-2-yl) acetamide (**7f11**)*

Started from **6f** and 2-aminopyrazine. White solid, 14 mg, yield = 53%. ^{1}H NMR (400 MHz, $CDCl_3$): δ 9.62 (s, 1H), 8.87 (s, 1H), 8.43 (s, 1H), 8.31 (s, 1H), 7.85 (dt, J = 8.8, 2.0 Hz, 2H), 7.65 (dd, J = 7.6, 0.8 Hz, 1H), 7.43 (td, J = 7.6, 1.2 Hz, 1H), 7.39–7.32 (m, 2H), 7.06 (dt, J = 9.2, 2.8 Hz, 2H), 4.75 (s, 2H) ppm. HPLC t_R = 8.68 min purity 98%; ESI-MS: 412.00 $[M+H]^+$.

4.3. Biology

4.3.1. Materials and methods

Dofetilide was synthesized in our own laboratory [33], and astemizole was purchased from Sigma Aldrich (Zwijndrecht, The Netherlands). Tritium-labeled dofetilide (specific activity 82.3 Ci $mmol^{-1}$) was purchased from PerkinElmer (Groningen, The Netherlands). Bovine serum albumin (BSA, fraction V) was purchased from Sigma (St. Louis, MO, USA). G418 was obtained from Stratagene (Cedar Creek, USA). All the other chemicals were of analytical grade and obtained from standard commercial sources. HEK293 cells stably expressing the K_v11.1 channel (HEK293K_v11.1) were kindly provided by Dr. Eckhard Ficker (University of Cleveland, USA).

4.3.2. Cell culture and membrane preparation

HEK293K_v11.1 cells were cultured, and membranes were prepared and stored as described previously [17].

4.3.3. Radioligand kinetic dissociation assays

Kinetic dissociation assays of $[^3H]$dofetilide were performed in incubation buffer (10 mM HEPES, 130 mM NaCl, 60 mM KCl, 0.8 mM $MgCl_2$, 1 mM EGTA, 10 mM glucose, 0.1% BSA, pH 7.4) as described previously with the following modifications [17]. Single point dissociation experiments were conducted by addition of 10 μM dofetilide in the absence (control) or presence of 10 μM synthesized compounds after preincubation at 25 °C for 2 h. After 6 min of dissociation, incubations were terminated by dilution with ice-cold wash buffer (25 mM Tris–HCl, 130 mM NaCl, 60 mM KCl, 0.8 mM $MgCl_2$, 0.05 mM $CaCl_2$, 0.05% BSA, pH 7.4). Separation of bound from free radioligand was performed by rapid filtration through a 96-well GF/B filter plate using a PerkinElmer Filtermate-harvester (PerkinElmer, Groningen, The Netherlands). The filter-bound radioactivity was determined by scintillation spectrometry using the P-E 1450 Microbeta Wallac Trilux scintillation counter (PerkinElmer) after addition of 25 μL Microscint and extraction. Full dissociation assays were carried out with 10 μM dofetilide in the absence (control) or presence of 50 μM selected compounds for a total period of 2 h after preincubation. The amounts of radioligand still bound to the receptor were measured at various time intervals. Concentration-dependent effects of compounds **7f** and **7p** were determined by addition of 10 μM dofetilide in the absence (control) or presence of different concentrations of **7f** and **7p**. After 6 min of dissociation, the incubations were terminated and samples were obtained as described above.

4.3.4. Radioligand displacement assay

$[^3H]$Dofetilide binding assays for the K_v11.1 channel were performed in incubation buffer as described previously [17]. Briefly, membrane aliquots containing 20 μg protein were incubated with 5 nM $[^3H]$dofetilide in a total volume of 100 μl incubation buffer at 25 °C for 1 h. Radioligand displacement experiments were carried out with various concentrations of tested compounds. Total binding was determined in the presence of incubation buffer, whereas nonspecific binding was evaluated with 10 μM astemizole. Incubations were terminated by dilution with ice-cold wash buffer, and samples were obtained as described in the "*radioligand kinetic dissociation assays*". The displacement assays of dofetilide and astemizole were conducted in the absence (control) or presence of 10 μM **7f**, **7h–j** and **7p**.

4.3.5. Data analysis

All data of radioligand binding assays were analyzed with Prism v. 5.0 (GraphPad, San Diego, CA, USA). Dissociation rate constants, k_{off}, were obtained by computer analysis of the exponential decay of $[^3H]$dofetilide bound to the K_v11.1 channel. EC_{50} values from kinetic dissociation assays were calculated by non-linear regression analysis of concentration–effect curves of dissociation in the presence of different concentrations of unlabeled ligands. IC_{50} values in displacement assays were directly obtained from non-linear regression analysis of dose–response curves. Apparent inhibitory binding constants (K_i values) were derived from the IC_{50} values according to the Cheng–Prusoff relationship [34]: $K_i = IC_{50}/(1 + [L^*]/K_D)$, where $[L^*]$ is the concentration of radioligand and K_D its dissociation constant from the saturation assay [31]. All values obtained from radioligand binding assays in this study are means of at least three independent experiments performed in duplicate, and data are presented as mean ± SEM. Statistical analysis was performed with a two-tailed unpaired Student's t-test.

Acknowledgments

Zhiyi Yu is supported by a scholarship from the Chinese Scholarship Council. The authors thank Dr. Julien Louvel for carefully checking and discussing the chemistry paragraphs in the main text and the SI.

Appendix A. Supplementary data

Supplementary data related to this article can be found at http://dx.doi.org/10.1016/j.ejmech.2015.10.032.

References

[1] L.T. May, K. Leach, P.M. Sexton, A. Christopoulos, Allosteric modulation of G protein-coupled receptors, Ann. Rev. Pharm. Toxicol. 47 (2007) 1–51.

[2] R.C. Hogg, B. Buisson, D. Bertrand, Allosteric modulation of ligand-gated ion channels, Biochem. Pharmacol. 70 (2005) 1267–1276.
[3] J.A. Lewis, E.P. Lebois, C.W. Lindsley, Allosteric modulation of kinases and GPCRs: design principles and structural diversity, Curr. Opin. Chem. Biol. 12 (2008) 269–280.
[4] A. Christopoulos, J.-P. Changeux, W.A. Catterall, D. Fabbro, T.P. Burris, J.A. Cidlowski, R.W. Olsen, J.A. Peters, R.R. Neubig, J.-P. Pin, P.M. Sexton, T.P. Kenakin, F.J. Ehlert, M. Spedding, C.J. Langmead, International union of basic and clinical pharmacology. XC. multisite pharmacology: recommendations for the nomenclature of receptor allosterism and allosteric ligands, Pharmacol. Rev. 66 (2014) 918–947.
[5] A.E. Davey, K. Leach, C. Valant, A.D. Conigrave, P.M. Sexton, A. Christopoulos, Positive and negative allosteric modulators promote biased signaling at the calcium-sensing receptor, Endocrinology 153 (2011) 1232–1241.
[6] M.C. Sanguinetti, M. Tristani-Firouzi, hERG potassium channels and cardiac arrhythmia, Nature 440 (2006) 463–469.
[7] J.I. Vandenberg, M.D. Perry, M.J. Perrin, S.A. Mann, Y. Ke, A.P. Hill, hERG K^+ channels: structure, function, and clinical significance, Physiol. Rev. 92 (2012) 1393–1478.
[8] A. Rayan, M. Falah, J. Raiyn, B. Da'adoosh, S. Kadan, H. Zaid, A. Goldblum, Indexing molecules for their hERG liability, Eur. J. Med. Chem. 65 (2013) 304–314.
[9] X. Xu, M. Recanatini, M. Roberti, G.-N. Tseng, Probing the binding sites and mechanisms of action of two human ether-a-go-go-related gene channel activators, 1,3-bis-(2-hydroxy-5-trifluoromethyl-phenyl)-urea (NS1643) and 2-[2-(3,4-dichloro-phenyl)-2,3-dihydro-1*H*-isoindol-5-ylamino]-nicotinic acid (PD307243), Mol. Pharmacol. 73 (2008) 1709–1721.
[10] M. Perry, M. Sanguinetti, J. Mitcheson, Revealing the structural basis of action of hERG potassium channel activators and blockers, J. Physiol. (Lond.) 588 (2010) 3157–3167.
[11] U. Ravens, Novel pharmacological approaches for antiarrhythmic therapy, Naunyn Schmiedeb. Arch. Pharmacol. 381 (2010) 187–193.
[12] M. Grunnet, R.S. Hansen, S.-P. Olesen, hERG1 channel activators: a new antiarrhythmic principle, Prog. Biophys. Mol. Biol. 98 (2008) 347–362.
[13] J. Kang, X. Chen, H. Wang, J. Ji, H. Cheng, J. Incardona, W. Reynolds, F. Viviani, M. Tabart, D. Rampe, Discovery of a small molecule activator of the human ether-a-go-go-related gene (HERG) cardiac K^+ channel, Mol. Pharmacol. 67 (2005) 827–836.
[14] M. Perry, F.B. Sachse, M.C. Sanguinetti, Structural basis of action for a human ether-a-go-go-related gene 1 potassium channel activator, Proc. Natl. Acad. Sci. U.S.A. 104 (2007) 13827–13832.
[15] S. Durdagi, J. Guo, J.P. Lees-Miller, S.Y. Noskov, H.J. Duff, Structure-guided topographic mapping and mutagenesis to elucidate binding sites for the human ether-a-go-go-related gene 1 potassium channel (KCNH2) activator NS1643, J. Pharmacol. Exp. Ther. 342 (2012) 441–452.
[16] R.S. Hansen, S.-P. Olesen, L.C.B. Rønn, M. Grunnet, In vivo effects of the I_{Kr} agonist NS3623 on cardiac electrophysiology of the guinea pig, J. Cardiovasc. Pharmacol. 52 (2008) 35–41.
[17] Z. Yu, E. Klaasse, L.H. Heitman, A.P. IJzerman, Allosteric modulators of the hERG K^+ channel: radioligand binding assays reveal allosteric characteristics of dofetilide analogs, Toxicol. Appl. Pharmacol. 274 (2014) 78–86.
[18] G. Seebohm, Activators of cation channels: potential in treatment of channelopathies, Mol. Pharmacol. 67 (2005) 585–588.
[19] H. Zhang, B. Zou, H. Yu, A. Moretti, X. Wang, W. Yan, J.J. Babcock, M. Bellin, O.B. McManus, G. Tomaselli, F. Nan, K.-L. Laugwitz, M. Li, Modulation of hERG potassium channel gating normalizes action potential duration prolonged by dysfunctional KCNQ1 potassium channel, Proc. Natl. Acad. Sci. U.S.A. 109 (2012) 11866–11871.
[20] T.G. Diness, Y.-H. Yeh, X.Y. Qi, D. Chartier, Y. Tsuji, R.S. Hansen, S.-P. Olesen, M. Grunnet, S. Nattel, Antiarrhythmic properties of a rapid delayed-rectifier current activator in rabbit models of acquired long QT syndrome, Cardiovasc. Res. 79 (2008) 61–69.
[21] X. Xu, J.J. Salata, J. Wang, Y. Wu, G. Yan, T. Liu, R.A. Marinchak, P.R. Kowey, Increasing I_{Ks} corrects abnormal repolarization in rabbit models of acquired LQT2 and ventricular hypertrophy, Am. J. Physiol. Heart Circ. Physiol. 283 (2002) H664–H670.
[22] F. Potet, A.N. Lorinc, S. Chaigne, C.R. Hopkins, R. Venkataraman, S.Z. Stepanovic, L.M. Lewis, E. Days, V.Y. Sidorov, D.W. Engers, B. Zou, D. Afshartous, A.L. George, C.M. Campbell, J.R. Balser, M. Li, F.J. Baudenbacher, C.W. Lindsley, C.D. Weaver, S. Kupershmidt, Identification and characterization of a compound that protects cardiac tissue from human ether-a-go-go-related gene (hERG)-related drug-induced arrhythmias, J. Biol. Chem. 287 (2012) 39613–39625.
[23] P.C. Ruenitz, C.S. Bourne, K.J. Sullivan, S.A. Moore, Estrogenic triarylethylene acetic acids: effect of structural variation on estrogen receptor affinity and estrogenic potency and efficacy in MCF-7 cells, J. Med. Chem. 39 (1996) 4853–4859.
[24] S. Breyer, A. Semmler, T. Miller, A. Hill, S. Geissler, U. Haberkorn, W. Mier, Radioiodinated dechloro-4-iodofenofibrate: a hydrophobic model drug for molecular imaging studies, Int. J. Pharm. 431 (2012) 78–83.
[25] H. Li, R. Zhu, W. Shi, K. He, Z. Shi, Synthesis of fluorenone derivatives through Pd-catalyzed dehydrogenative cyclization, Org. Lett. 14 (2012) 4850–4853.
[26] B. Li, T.V. Magee, R.A. Buzon, D.W. Widlicka, D.R. Bill, T. Brandt, X. Cao, M. Coutant, H. Dou, K. Granskog, M.E. Flanagan, C.M. Hayward, B. Li, F. Liu, W. Liu, T.-T. Nguyen, J.W. Raggon, P. Rose, J. Rainville, U.D. Reilly, Y. Shen, J. Sun, G.E. Wilcox, Process development of a novel azetidinyl ketolide antibiotic, Org. Process Res. Dev. 16 (2012) 788–797.
[27] E. Kostenis, K. Mohr, Two-point kinetic experiments to quantify allosteric effects on radioligand dissociation, Trends Pharmacol. Sci. 17 (1996) 280–283.
[28] M. Kalinichev, T. Donovan-Rodriguez, F. Girard, E. Riguet, M. Rouillier, B. Bournique, H. Haddouk, V. Mutel, S. Poli, Evaluation of peripheral versus central effects of $GABA_B$ receptor activation using a novel, positive allosteric modulator of the $GABA_B$ receptor ADX71943, a pharmacological tool compound with a fully peripheral activity profile, Br. J. Pharmacol. 171 (2014) 4941–4954.
[29] Z. Gao, J.E. Van Muijlwijk-Koezen, A. Chen, C.E. Müller, A.P. IJzerman, K.A. Jacobson, Allosteric modulation of A_3 adenosine receptors by a series of 3-(2-pyridinyl) isoquinoline derivatives, Mol. Pharmacol. 60 (2001) 1057–1063.
[30] A.M. van den Nieuwendijk, D. Pietra, L. Heitman, A. Göblyös, A.P. IJzerman, Synthesis and biological evaluation of 2, 3, 5-substituted [1, 2, 4] thiadiazoles as allosteric modulators of adenosine receptors, J. Med. Chem. 47 (2004) 663–672.
[31] Z. Yu, A. IJzerman, L. Heitman, K_v11.1 (hERG)-induced cardiotoxicity: a molecular insight from a binding kinetics study of prototypic K_v11.1 (hERG) inhibitors, Br. J. Pharmacol. 172 (2015) 940–945.
[32] G. Szabo, V. Farkas, M. Grunnet, A. Mohacsi, P.P. Nanasi, Enhanced repolarization capacity: new potential antiarrhythmic strategy based on HERG channel activation, Curr. Med. Chem. 18 (2011) 3607–3621.
[33] Shagufta, D. Guo, E. Klaasse, H. de Vries, J. Brussee, L. Nalos, M.B. Rook, M.A. Vos, M.A. van der Heyden, A.P. IJzerman, Exploring chemical substructures essential for hERG K^+ channel blockade by synthesis and biological evaluation of dofetilide analogues, ChemMedChem 4 (2009) 1722–1732.
[34] Y. Cheng, W.H. Prusoff, Relationship between the inhibition constant (K_I) and the concentration of inhibitor which causes 50 percent inhibition (I_{50}) of an enzymatic reaction, Biochem. Pharmacol. 22 (1973) 3099–3108.